AD-E100 148

(1) LEVEL II

(9) Status Report. 1 Apr 74-Jan 76,

(6) PASSIVE SPACE COMMUNICATION ARRAY.

(10) William A. EDSON

(11) Feb 76

(12) 56p.

Prepared for:

DEFENSE COMMUNICATIONS AGENCY
WASHINGTON, D.C. 20305

CONTRACT (15) DCA100-74-C-0035, // ARPA Order-2645

(18) SBIE

(19) AD-E100 148

Sponsored by

DEFENSE ADVANCED RESEARCH PROJECTS AGENCY
ARPA ORDER 2645

SRI
STANFORD RESEARCH INSTITUTE
Menlo Park, California 94025 · U.S.A.

STANFORD RESEARCH INSTITUTE
Menlo Park, California 94025 · U.S.A.

Status Report *February 1976*

PASSIVE SPACE COMMUNICATION ARRAY

By: W. A. EDSON

Prepared for:

DEFENSE COMMUNICATIONS AGENCY
WASHINGTON, D.C. 20305

CONTRACT DCA100-74-C-0035

SRI Project 3323

Approved by:

DAVID A. JOHNSON, *Director*
Radio Physics Laboratory

RAY L. LEADABRAND, *Executive Director*
Electronics and Radio Sciences Division

ORIGINAL CONTAINS COLOR PLATES: ALL DDC REPRODUCTIONS WILL BE IN BLACK AND WHITE

Copy No. 68

SECURITY CLASSIFICATION OF THIS PAGE (When Data Entered)

REPORT DOCUMENTATION PAGE		READ INSTRUCTIONS BEFORE COMPLETING FORM
1. REPORT NUMBER	2. GOVT ACCESSION NO.	3. RECIPIENT'S CATALOG NUMBER
4. TITLE (and Subtitle) PASSIVE SPACE COMMUNICATION ARRAY		5. TYPE OF REPORT & PERIOD COVERED Status Report Covering the period 1 April 1974 through January 1976
		6. PERFORMING ORG. REPORT NUMBER SRI Project 3323
7. AUTHOR(s) William A. Edson		8. CONTRACT OR GRANT NUMBER(s) Contract DCA100-74-C-0035
9. PERFORMING ORGANIZATION NAME AND ADDRESS Stanford Research Institute 333 Ravenswood Avenue Menlo Park, California 94025		10. PROGRAM ELEMENT, PROJECT, TASK AREA & WORK UNIT NUMBERS
11. CONTROLLING OFFICE NAME AND ADDRESS Defense Communications Agency Washington, D.C. 20305		12. REPORT DATE February 1976 13. NO. OF PAGES 64
14. MONITORING AGENCY NAME & ADDRESS (if diff. from Controlling Office)		15. SECURITY CLASS. (of this report) Unclassified 15a. DECLASSIFICATION/DOWNGRADING SCHEDULE N/A

16. DISTRIBUTION STATEMENT (of this report)

Approved for public release
distribution unlimited.

17. DISTRIBUTION STATEMENT (of the abstract entered in Block 20, if different from report)

18. SUPPLEMENTARY NOTES

19. KEY WORDS (Continue on reverse side if necessary and identify by block number)

Satellite communications
Jam-resistant
Space array
Passive satellite

SRI carried

20. ABSTRACT (Continue on reverse side if necessary and identify by block number)

Under a project monitored by DCA and funded by ARPA, SRI is carrying out a project to demonstrate the feasibility of a passive array-type satellite for long-distance survivable communication. The demonstration satellite will consist of approximately 10,000 aluminum spheres one centimeter in diameter arranged in a linear array. The array will be held straight and vertical by gravity-gradient forces at synchronous altitude. It will operate at frequencies near 10 GHz.

DD FORM 1 JAN 73 1473
EDITION OF 1 NOV 65 IS OBSOLETE

iii

SECURITY CLASSIFICATION OF THIS PAGE (When Data Entered)

19. KEY WORDS (Continued)

20 ABSTRACT (Continued)

The array has the properties of a passive linear circuit and is completely free from intermodulation or harmonic generation. These features, in combination with the fact that the return may be directed or steered by choice of the operating frequency, provide the communication link with privacy and a high degree of jam resistance. The most probable launch is as a piggyback load accompanying a pair of 777 satellites on a Titan III-C booster late in 1977.

Consideration has gone into both the mechanical and electromagnetic properties of such an array. Experiments have confirmed that the electromagnetic scattering properties of the array are consistent with theoretical results. The orbital dynamics of the array have been investigated, and techniques for deploying such a structure have been developed.

To obtain complete verification of the performance of the passive space array it will be necessary to launch a demonstration unit into orbit. Project effort is currently being concentrated upon activities directly leading to such a launch.

CONTENTS

ILLUSTRATIONS

TABLES

I INTRODUCTION

The usefulness of satellites for both communication and navigation applications is now established beyond doubt. A great variety of satellites are in current use, and additional satellites for a variety of purposes are being prepared and launched. All of the satellites in current use are active in the sense that they either amplify signals delivered to them from an earth station or independently generate signal power.

Passive satellites that provide a communication channel by reflecting earth-originated signals have been investigated in the past--for example through the Echo and West Ford experiments. However, no operational system has resulted from this work. The present project is concerned with a new form of satellite that shows promise for meeting certain special communication requirements. Figure 1 is an artist's conception of a transatlantic communication link using a satellite of this kind. Signals transmitted toward the satellite from Europe are returned to a receiving station in the United States.

The basic principles that underlie this work are due to Joseph C. Yater* and were presented in a 1972 technical paper[1]† and his U.S. Patent of 1969.[2] This satellite differs from previous passive satellites in that it consists of a large number of scattering elements, arranged in an orderly array that results in coherent addition of scattered energy to form the return signal. The principles that govern the array operation are presented in Figure 2. The signal returned to earth is concentrated in a

---

*Mr. Yater is supporting this project as a consultant to SRI.

†References are listed at the end of this report.

thin, walled hollow cone that inersects the earth in a limited circular pattern centered on the subsatellite point. Varying the wavelength of the signal changes the radius of this circle. Only one lobe is returned to earth if the array spacing lies in the range between $\lambda/2$ and λ.

It is emphasized that the coverage and orbital properties of this satellite are essentially the same as those of the synchronous satellites. The principle difference is the absence of active elements in the array, with the resulting implications of simplicity, economy, survivability, jam resistance, reliability, and long life. The orbital characteristics are governed by the fact that the mass-to-projected-surface area of the array is smaller than is typical of active satellites.

Aluminum spheres have been chosen as the basic element of the array because they meet several independent criteria. Of all shapes, the sphere has the smallest surface area for a given volume and hence mass. This is desirable for orbital reasons. From the electrical viewpoint the sphere is desirable for several reasons. A resonant sphere is a broadband scattering element. Therefore, the behavior of each individual sphere is quite insensitive to frequency. Also, the scattering properties are completely independent of the direction from which the signal arrives, so the scattered signal is returned almost equally in all directions. Aluminum is the preferred metal because it resists vaporization by x-rays, is durable, easy to work, and has an appropriate density.

Gravity-gradient forces are used to hold the array straight and aligned with the local vertical, as required for the desired electrical operation. Unfortunately, gravity-gradient forces are very weak. The greatest tension in the array, which occurs at the center, is about 0.5 mg--i.e., about 1/50,000 oz, and about one hundred times smaller than the weight of an ordinary paper-fastening staple. It is therefore necessary to take great care to preserve straightness and orbital stability. Also,

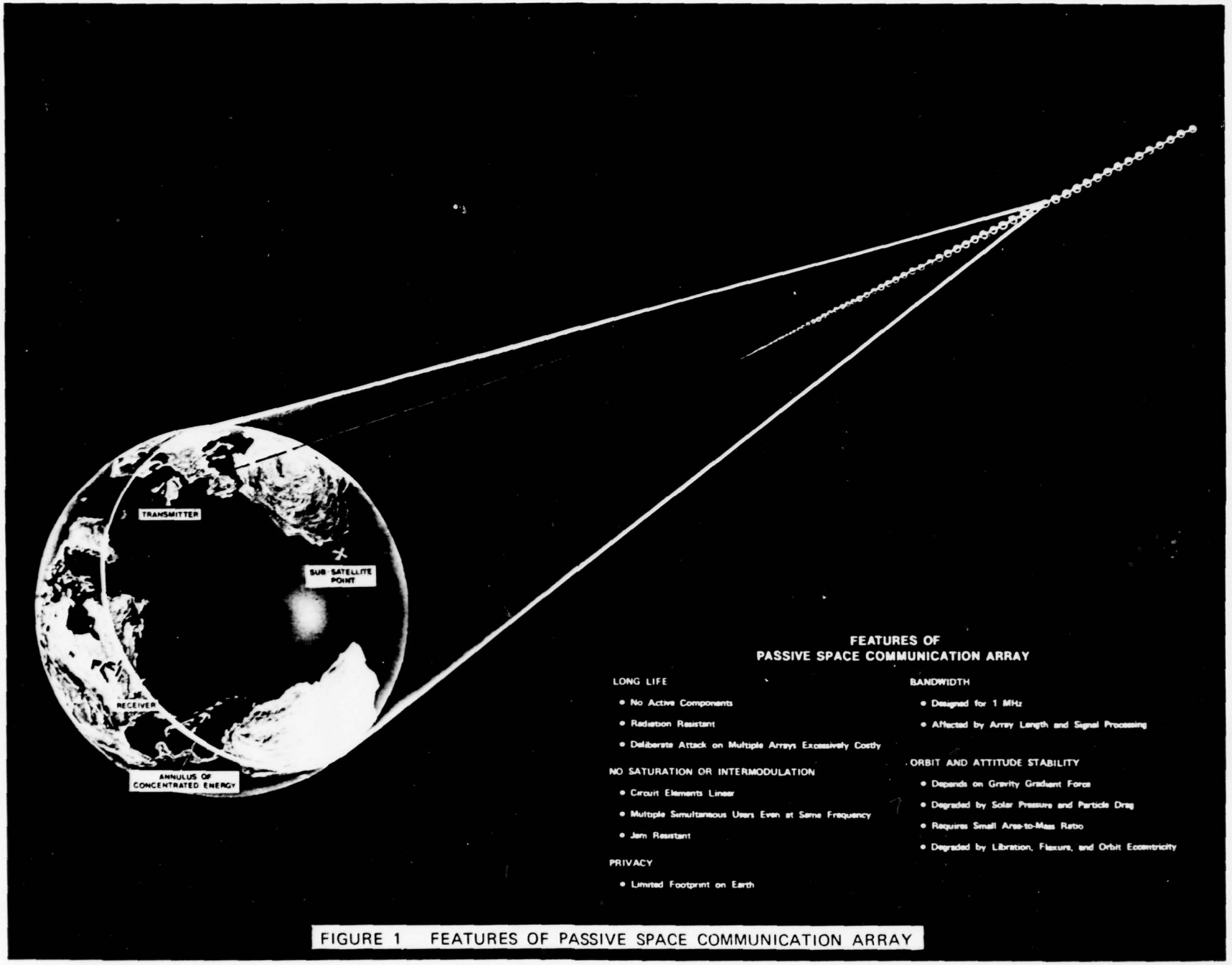

FIGURE 1 FEATURES OF PASSIVE SPACE COMMUNICATION ARRAY

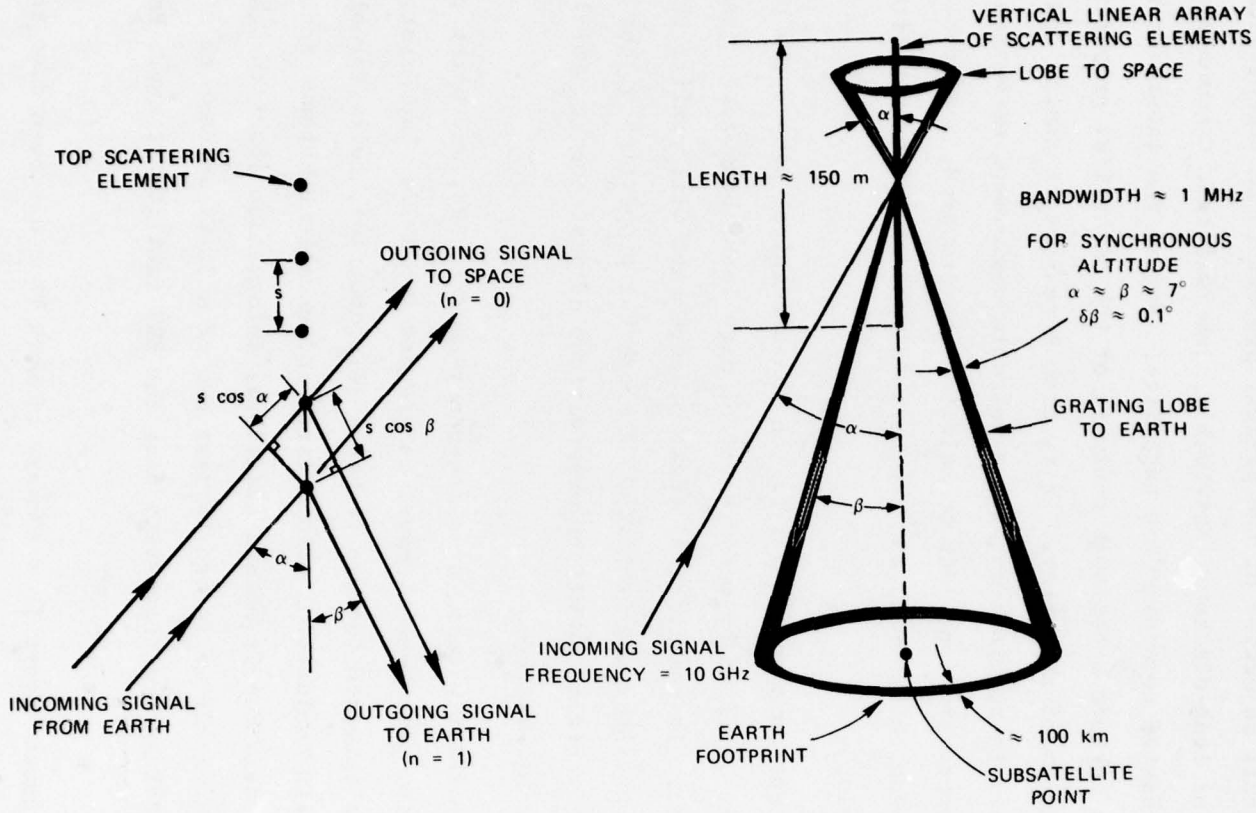

FIGURE 2 RESPONSE OF A COLUMNAR ARRAY OF ISOTROPIC SCATTERERS

the deployment of such a structure presents problems that differ from those that have been solved in connection with existing satellites.

The overall objective of the present project is to demonstrate the feasibility of long-distance, survivable, jam-resistant communication by means of a passive communication satellite. Before the launch it has been necessary to perform a thorough analysis of the electrical properties and orbital dynamics of the array. It is also necessary to design and fabricate the array in combination with a suitable deployment mechanism. Furthermore, ground stations must be selected and prepared, a launch assignment must be secured, and the payload must be integrated with the launch vehicle.

Subsequent to a successful launch the electrical properties of the array must be verified by measurement of path loss, beamwidth, bandwidth, and sidelobes. In combination, these measurements will confirm the desired frequency-steering property. The orbital properties of the array will also be verified by direct observations of position and inferred observations of attitude.

The feasibility test, at a frequency near 10 GHz, and using the Haystack facility near Boston, Mass. is planned for 1977. The Haystack facility was selected because it has a very powerful, fully tunable transmitter in conjunction with a large and excellent antenna and a very sensitive receiver. To obtain additional information about the characteristics of the array we intend to make use of a 30-ft antenna as a receive-only site at Stanford University near the SRI facility at Menlo Park, California.

The present report is a summary of work that has been done in a period exceeding two years. Much additional detail is available in the individual reports cited in the list of references at the end.

II ELECTRICAL PROPERTIES OF THE ARRAY

As indicated in Figure 2, the demonstration array consists of 10,000 spherical conductive scattering elements arranged in a straight line. The diameter of each sphere is one centimeter, corresponding to resonance at frequencies near 10 GHz--i.e., wavelengths near 3 cm. The center-to-center spacing, s, is 1.51 cm, slightly larger than one-half wavelength. The following paragraphs develop the equations that describe the scattering behavior of such an array and derive equations for signal strength, beam pattern, and frequency-steering properties.*

A. Grating Equation

An array of isotropic scattering elements uniformly spaced in a single column is shown in Figure 2. To produce maximum signal strength, the energy scattered by each element must add in phase at the receiving site; or, equivalently, the raypaths shown must differ in length from each other by an integral number of wavelengths. Expressed mathematically, this requirement becomes

$$s \cos \alpha + s \cos \beta = n\lambda = n\frac{c}{f} \qquad (1)$$

---

*The remainder of this section is abstracted from an earlier report on this project,[3] which contains more detailed information. In particular, it derives path-loss values and develops tradeoffs between array length, bandwidth and signal-processing techniques that are related to pulse compression radar.

where

n = An integer

f = Frequency

c = Speed of light

λ = Wavelength

and the symbols s, α, and β are identified in Figure 2.

To provide private communication it is desirable that only one transmission (grating) lobe return to earth. This condition is met if $\lambda/2 < s < \lambda$, so that n = 1 is the only positive integer for which the above equation is satisfied.

B. Frequency Steering

In normal situations the transmitting site and hence the incidence angle, α, as well as the interelement spacing, s, of the array must be chosen a priori. It is still possible to vary the signal return angle, β, by changing the frequency of transmission, as can be seen by solving for this angle in Eq. (1):

$$\beta = \cos^{-1}\left[\frac{c}{fs} - \cos\alpha\right] \quad . \tag{2}$$

This equation shows that the returned signal can be "steered" by varying f, thus allowing the transmitter to communicate with receiving sites located on different circles about the subsatellite point [see Figure 2(b)].

For a small change in frequency (or wavelength), the change in outgoing angle of the signal is obtained by differentiating Eq. (1) with respect to f, which gives

$$\frac{\partial \beta}{\partial f} = \frac{\cos \alpha + \cos \beta}{f \sin \beta} \quad . \tag{3}$$

This is the rate of steering vs frequency change.

C. Beamwidth and Earth Footprint

For any fixed value of α, the beamwidth or angular spread, $\delta\beta$, in the outgoing beam in Figure 2(b) is obtained as follows. Assume that the contribution from each isotropic reflector is in phase at the center of the grating lobe. The first null in the diffraction pattern describing the lobe arises when an additional wavelength of phase shift accumulates across the total length of the array. That is,

$$(L + s) \cos \alpha + (L + s) \cos (\beta \pm \delta\beta_o) = N\lambda \mp \lambda \tag{4}$$

where N is the number of elements in the column. Making use of a trigonometric identity and saving the leading term of a trigonometric expansion with argument $\delta\beta_o$ (for $\delta\beta_o \ll 1$ radian) gives

$$\delta\beta_o = \frac{\lambda}{(L + s) \sin \beta} \text{ (radians)} \tag{5}$$

as the half-beamwidth to the first null in the beam pattern. The full beamwidth to the half-power points is 88.6% of $\delta\beta_o$;* hence,

$$\delta\beta = \frac{0.886\,\lambda}{(L + s) \sin \beta} \text{ (radians)} \quad . \tag{6}$$

---

*This is a result of the (sin x)/(x) radiation pattern of the array.

Similarly, the half-power beamwidth of the undesired upgoing beam, which is due to "specular" scattering from the column, is given by

$$\delta\alpha = \frac{0.886\,\lambda}{(L + s)\sin\alpha} \quad \text{(radians)} \quad . \tag{7}$$

D. Bandwidth

The effects of beamwidth and dispersion determine the bandwidth capability of the linear columnar array. Combining Eqs. (3) and (6) with the identity $c = f\lambda$ gives the half-power bandwidth, δf:

$$\delta f = \frac{f \sin\beta}{\cos\alpha + \cos\beta}\,\delta\beta = \frac{0.886\,f}{N} = \frac{0.886\,c}{(L + s)(\cos\alpha + \cos\beta)} \quad . \tag{8}$$

In all cases of present interest this result is closely approximated by the simpler expression

$$\delta f = 0.886\,c/L \quad . \tag{8a}$$

E. Gain

To calculate the gain of the array, we use a standard expression from antenna theory.[4] In words, this formula states that the gain of an antenna is 4π steradians divided by the total solid angle subtended by the antenna half-power radiation pattern. That is,

$$G = \frac{4\pi}{(\text{pattern solid angle})} \quad . \tag{9}$$

The gain of the columnar array is given, to an accuracy of better than one percent, by the expression

$$G = \frac{4\pi}{2\pi \sin\alpha\,\delta\alpha + 2\pi \sin\beta\,\delta\beta} \quad , \tag{10}$$

which neglects sidelobes in the array pattern, because they are at least 13 dB weaker than the two main lobes. Assuming $\alpha \approx \beta$ and substituting Eqs. (5) and (6) into Eq. (10) gives:

$$G = \frac{(L + s)}{0.886\ \lambda} \approx \frac{Ns}{0.886\ \lambda} \approx \frac{L}{0.886\ \lambda} \quad . \tag{11}$$

F. Array Radar Cross Section

If a receiving antenna remains resonant over the operating frequency range (i.e., if the impedance seen at the antenna terminals is purely resistive at those frequencies), the effective area of the antenna is given by the formula[4]

$$A_e = \frac{\lambda^2}{4\pi} G \quad . \tag{12}$$

If the terminals of such a resonant receiving antenna are short-circuited in order to create a reflecting or scattering structure (as is done in the space array), the resulting scattering area (A_s) of the antenna is:[4]

$$A_s = 4A_e = \frac{\lambda^2}{\pi} G \quad . \tag{13}$$

The radar cross section (σ) of the shorted antenna is now obtained by using

$$\sigma = A_s \cdot G \quad . \tag{14}$$

For the case of the columnar array of isotropes, the "resonant" constraint is always satisfied and the expressions for A_s and G may be substituted in Eq. (14) to give

$$\sigma = \frac{\lambda^2}{\pi}\left[\frac{L + s}{0.886\,\lambda}\right]^2 = (0.41)(L + s)^2 \approx (0.41)\,L^2 \qquad (15)$$

where the approximation is valid for $L \gg s$.

The formulas derived above are exact for a column of isotropic elements. They apply with little error to a column of spheres because the scattering properties of a resonant sphere are nearly isotropic.

G. Measurements

The values of bandwidth, beamwidth, and radar cross section derived in the preceding sections of this chapter have been confirmed by experiments. For arrays consisting of less than about one hundred spheres it was practical to make measurements in our anechoic chamber,[3] which has dimensions of approximately 7 by 10 by 18 ft. For an array of 1,000 elements this approach was impractical, and measurements were made by suspending the array from a manned hot-air balloon[5] at an elevation of approximately 1500 ft.

By careful choice of a time when the air was very calm and by careful attention to the instrumentation, it was possible to obtain accurate measurements, which are in good agreement with theory. Figure 3, reproduced from Ref. 5, summarizes the results obtained. In anticipation of the following section it is noted that although differing in detail, the measured sidelobes are not substantially stronger than those predicted.

The measurement of 1,000 elements, though possible, was difficult. No plausible experiment on or near the surface of the earth will measure the signal return, bandwidth, beamwidth, frequency steering, and sidelobes characteristics of an array of 10,000 elements. Experimental verification of these parameters is therefore an important goal of the feasibility demonstration experiment.

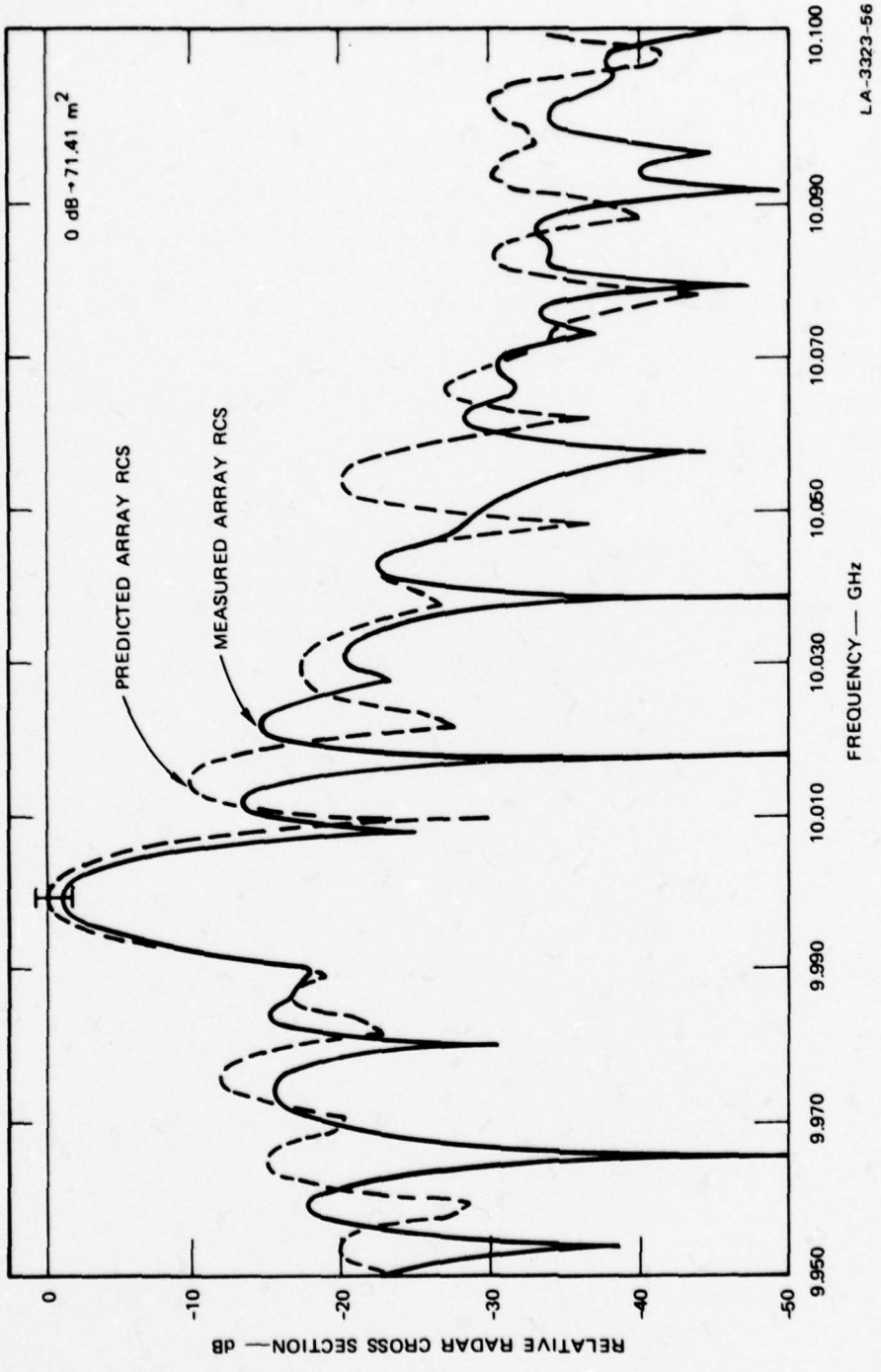

FIGURE 3 COMPARISON OF PREDICTED AND MEASURED ARRAY RCS AS A FUNCTION OF FREQUENCY

III PRIVACY AND RESISTANCE TO JAMMING

An important feature of the space array is that it provides a considerable degree of privacy against interception by an undesired listener and also gives a comparable degree of resistance to jamming injected by an opponent who wishes to interfere with the communication path. These advantages result from the fact that the array itself is electrically linear and that the earth footprint contains a relatively small area.

Jammers carried by balloons, aircraft, drones, rockets, or low-orbit satellites operate by injecting their signals directly into the main beam of the receiving antenna. This jamming mode would be effective, but would face serious operational difficulties. A jammer carried by a synchronous satellite located near the space array could be marginally effective as indicated by the following calculation. Suppose that the jammer radiates 10 watts. It must cover a considerable frequency band (e.g., 50 MHz) to deny use of the satellite over the geometric paths that are likely to be used. It must have a total beamwidth of about 8° to cover credible ground stations. The latter figure limits the gain to about 27 dB. Therefore the power density at the earth is +10 + 27 - 163 - 77 dBW/Hz where the four terms (in dB notation) represent the power generated, the antenna gain, the geometrical speeding factor, and the spectrum spreading factors, respectively. The net result is -203 dBW/Hz--only one dB above thermal noise at 300° K. Such a jammer would be considerably more complicated and expensive than the array, and is therefore not regarded as cost-effective.

Because of earth curvature no earth-based jammer can inject its signal directly into the receiving antenna. Therefore, the jammer must

radiate the same frequency as that used for communicating, and the jammer is forced to work through the array.

Because the array is passive and linear it cannot be caused to saturate and thereby produce harmonics or intermodulation. Consequently, a jammer can be effective only by transmitting at a frequency within the pass band of the receiving station. Practical receivers provide a very high degree of rejection to signals outside the intended pass band. Therefore, the frequency chosen for communicating, and hence the frequency that must be adopted by the jammer, is controlled by the spacing, location, and attitude of the array, and by the location of the intended receiver. The situation may be visualized by reference to Figure 4. Unless the jammer is located upon the annulus that passes through the transmitter, the jamming signal returned by the array will form an annulus that does not intersect the receiver. Therefore the jammer is forced to work through a sidelobe of the array. It is for this reason that the sidelobe behavior of the array is of great importance.

With the 10,000-element array to be used in the feasibility demonstration, the transmitting (or receiving) annulus has a 3-dB width of approximately 100 km. However, with the longer array contemplated for future systems, the width of this annulus will shrink to approximately 10 km.

For a perfectly uniform array the distribution of the electric field of the signal returned to the earth has a sin x/x distribution along any radial through the subsatellite point that crosses the favored annulus. The convergence of this function is illustrated in Figure 5.

Because the array is located at a great distance from the earth, it follows that all path lengths are nearly equal. Therefore the field strength of the received signal is virtually independent of the location of the transmitting and receiving antennas, and can be controlled by the power radiated by the transmitter. By the use of error-correcting codes

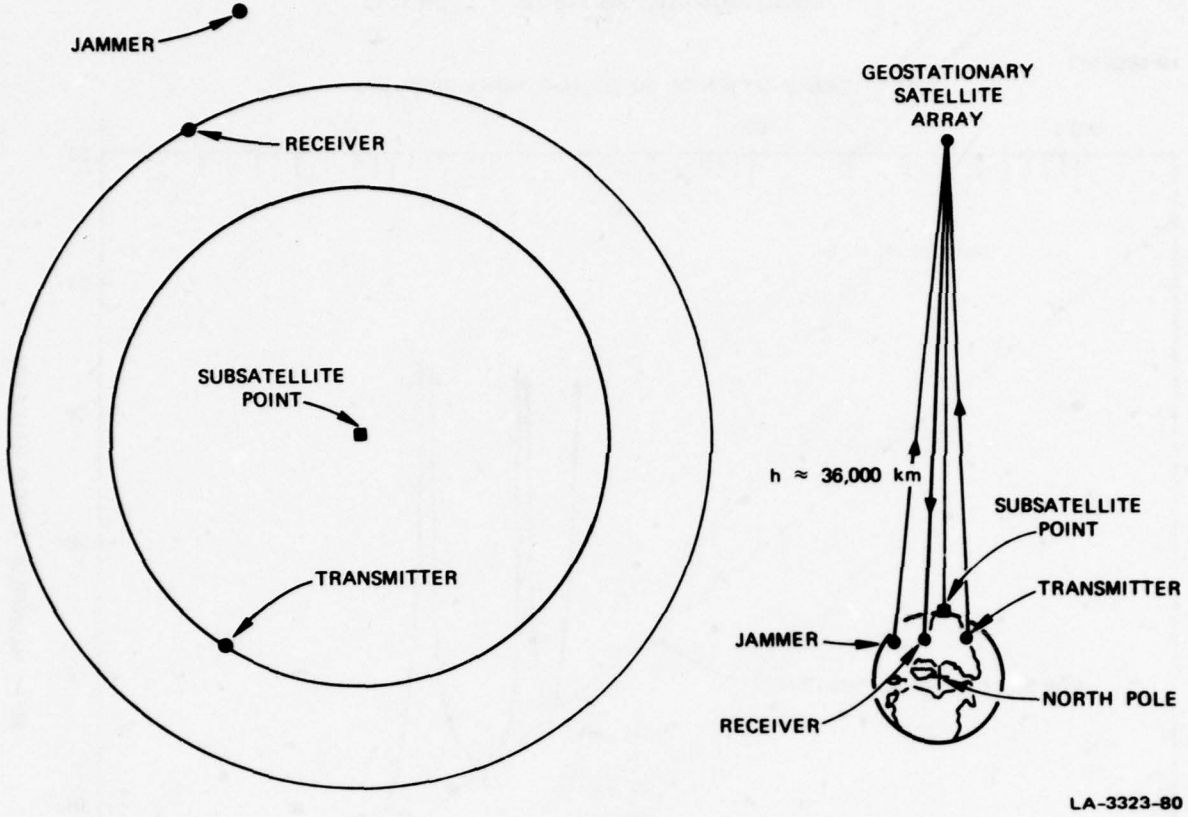

FIGURE 4 JAMMING GEOMETRY

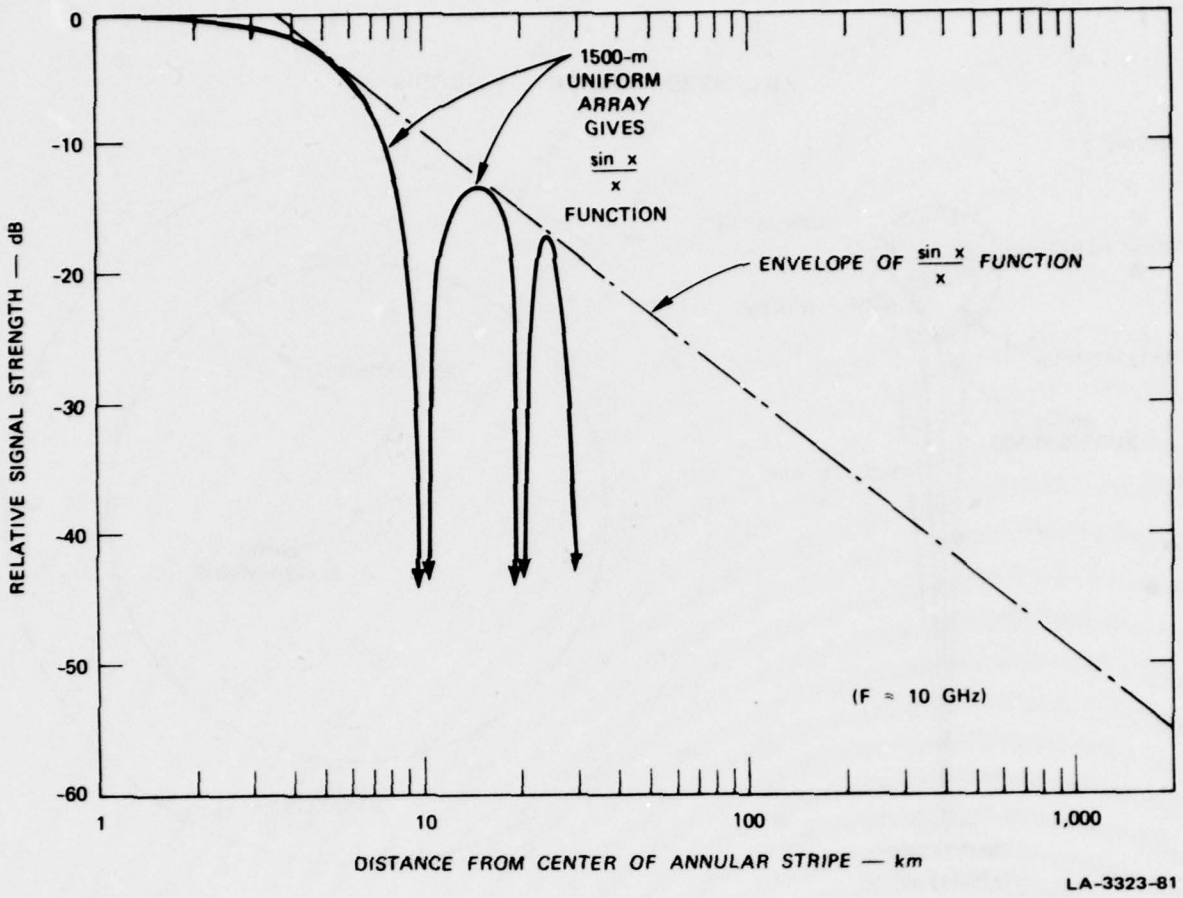

FIGURE 5 SIDELOBE DISTRIBUTIONS

it is possible to obtain very low error rates with signal-to-noise ratios (SNRs) in the neighborhood of 10 dB. When error-correcting codes are used, the jamming power must come within about 5 dB of the normal received power in order to produce serious interference. On this basis we can estimate the power and antenna requirements of the jammer.

Consider the situation in which an earth-based jammer is working against an airborne transmitter. Consistent with Section IV, we assume that the airborne system radiates 10 kW through a 5-ft parabolic antenna, and that the earth-based jammer radiates 1 MW through a 50-ft antenna. These assumptions are quite favorable to the jammer in that they pit a powerful earth-based transmitter with a large antenna against a modest airborne transmitter with a much smaller antenna. In this situation the jammer has an advantage of 20 dB in power, plus 20 dB in antenna gain, plus 5 dB in signal power requirement, for a total of 45 dB. To defeat such a jammer the array must provide a sidelobe discrimination of at least 45 dB. Inspection of Figure 5 indicates that this condition is met if the jammer is more than 1000 km from the annulus that passes through the transmitter (Figure 4).

The margin against the jammer can be increased by making use of spread-spectrum signals. However, difficulties of initiating communication and maintaining synchronization reduce this advantage in practical systems.

The jamming and interception problems are both affected in a way favorable to the intended user and unfavorable to the opponent by either libration or east-west drift of the satellite. This is true because the transmitting frequency can be adjusted by the intended user to maintain favorable transmission properties in the face of either of these disturbances. In contrast, the opponent is faced with time-variable conditions that require movement of the transmitting apparatus through substantial distances--a requirement difficult to meet.

In practical antennas, the sidelobe pattern is strongly affected by mechanical imperfections. It seems probable that the same statement will apply to practical arrays. The sidelobe pattern is the dominant parameter in determining system resistance to jamming. Therefore an important objective of the feasibility demonstration experiment is to measure the sidelobe levels actually achieved.

IV SYSTEM APPLICATIONS AND TRADEOFFS

A. The Signal-to-Noise Ratio

The rate at which information can be relayed by means of a passive satellite array depends on the construction of the array, the operating frequency, the size of the transmitting and receiving antennas, the transmitter power, and the receiver noise figure.

The distance R from a geostationary satellite to an earth station is nearly the same for all points visible from the satellite. Therefore, a single value of R can be used in the standard radar equation to calculate the power P_r received by a ground station. For free-space conditions this equation may be written:

$$P_r = \frac{P_t G_t}{4\pi R^2} \frac{\sigma}{4\pi R^2} A_r \qquad (16)$$

where

P_t = Transmitter power

G_t = Transmitter antenna gain

σ = Radar cross section (RCS) of the satellite

A_r = Effective aperture of the receiver antenna

G_r = Receiver antenna gain

R = Altitude = 36,000 km.

The receiver noise power is given by

$$P_n = kT\,\delta f \qquad (17)$$

where

P_n = Noise power at receiver input

k = Boltzmann's constant

T = System noise temperature

δf = Receiver bandwidth.

Substitution of numerical values in Eq. (15) of Section II ($\sigma = 0.41 L^2$) yields $\sigma \approx 10^4$ for the 150 meter array to be used initially and $\sigma \approx 10^6$ for the 1500 meter array planned for operation systems. If we substitute $\sigma = 10^6$, and select 7.5 GHz as a suitable operating frequency, we may design a two-way teletype system having the parameters shown in Table 1. Although identified with an air-to-ground link, these parameters may also be applied with little change to a ship-to-shore or ship-to-ship communication system.

B. Frequency Tradeoffs

As noted in Eq. (15), the radar cross section of our satellite is independent of wavelength and is proportional to the square of the array length. For a given diameter of the transmitting antenna the gain is proportional to the frequency squared. These are the two dominant considerations in selection of the operating frequency and array length. The other important fact is that the bandwidth limitation of the array varies inversely with the array length.

Use of the highest practical microwave frequency is indicated by the facts that the size of the scattering elements and hence the weight of the array tend to decrease with increasing frequency, and that the gain of a particular transmitting antenna tends to increase with frequency. On the other hand, a lower frequency is indicated by the surface tolerance requirements on antennas, the ease and convenience with which power can be

Table 1

TENTATIVE CONFIGURATION FOR A TWO-WAY TELETYPE SYSTEM

Airborne-to-ground and vice versa (via space-array satellite)
Array length--1500 m
Operating frequency--7.5 GHz
Airborne-antenna aperture--5 ft
Ground-antenna aperture--30 ft
Proliferated, hidden, transportable, and/or hardened ground antennas for MEECN (limited antenna steering required)
Transmitter power--1.5 kW for 100 Hz bandwidth
Array bandwidth--100 kHz (spread-spectrum potential--30 dB processing gain)
Receiver noise temperature--150° K
Viterbi decoder
Error rate--10^{-10}
SNR--6.7 → 8.2 dB

generated, and the ease of realizing low values of receiver noise figure. Moreover, reliability of transmission is seriously reduced by attenuation caused by rain and other atmospheric disturbances if the frequency is increased much above 10 GHz. Frequencies between about 6 and 12 GHz are attractive as a practical compromise between these various considerations. A frequency of 7.5 GHz has already been suggested as a suitable value.

C. Array-Length Tradeoffs

The effect of varying the array length is shown in Figure 6. For an array of fixed length the SNR can be improved simply by narrowing the bandwidth of the receiver and reducing the information bandwidth. Alternatively, the array length can be increased and the receiving bandwidth correspondingly

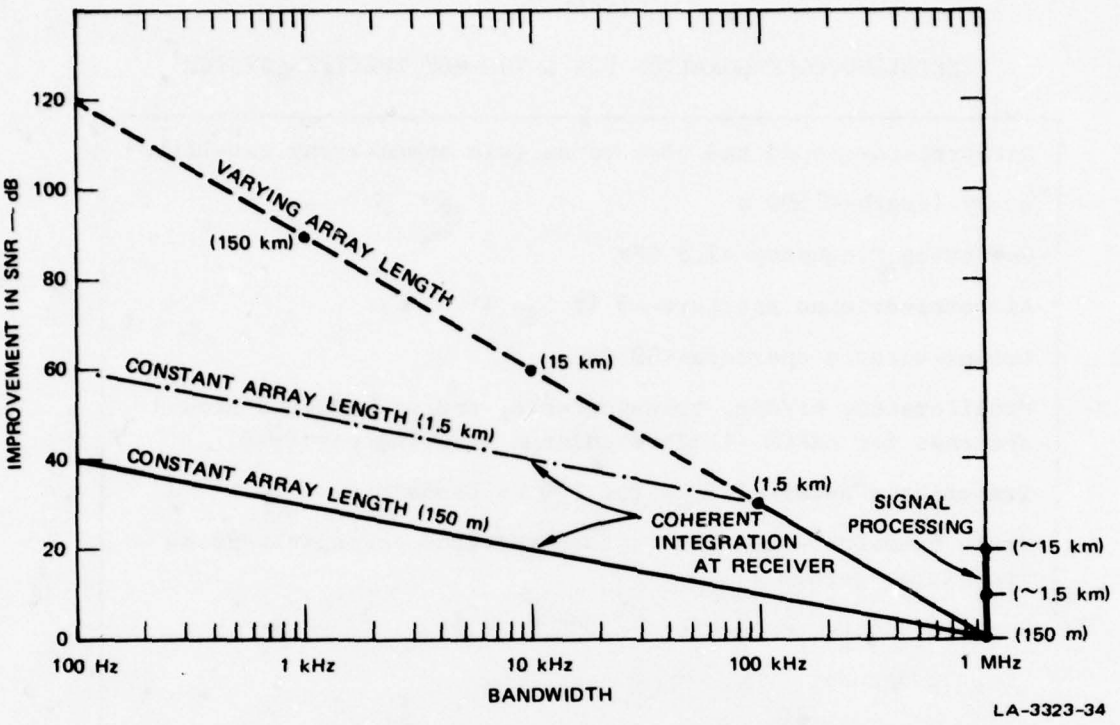

FIGURE 6 SNR/BANDWIDTH TRADEOFFS

reduced. This procedure increases the radar cross section of the array while reducing receiver noise power. As a result, the system SNR improves at the rate of 30 dB per decade of bandwidth. Finally, it is possible to increase the received SNR without reducing the bandwidth, by increasing the array length, modifying the array configuration, and using corresponding signal processing such as that used in pulse-compression radars. Additional information on tradeoffs is provided in Figure 7.

D. Two-Way Communication

Active satellites employ different frequencies in the uplinks and downlinks to simplify the problem of multiplexing the signals to provide two-way communication. In a single, passive array this procedure is impossible because the return signal is necessarily at the same frequency as the transmitter signal. To provide full-duplex two-way communication,

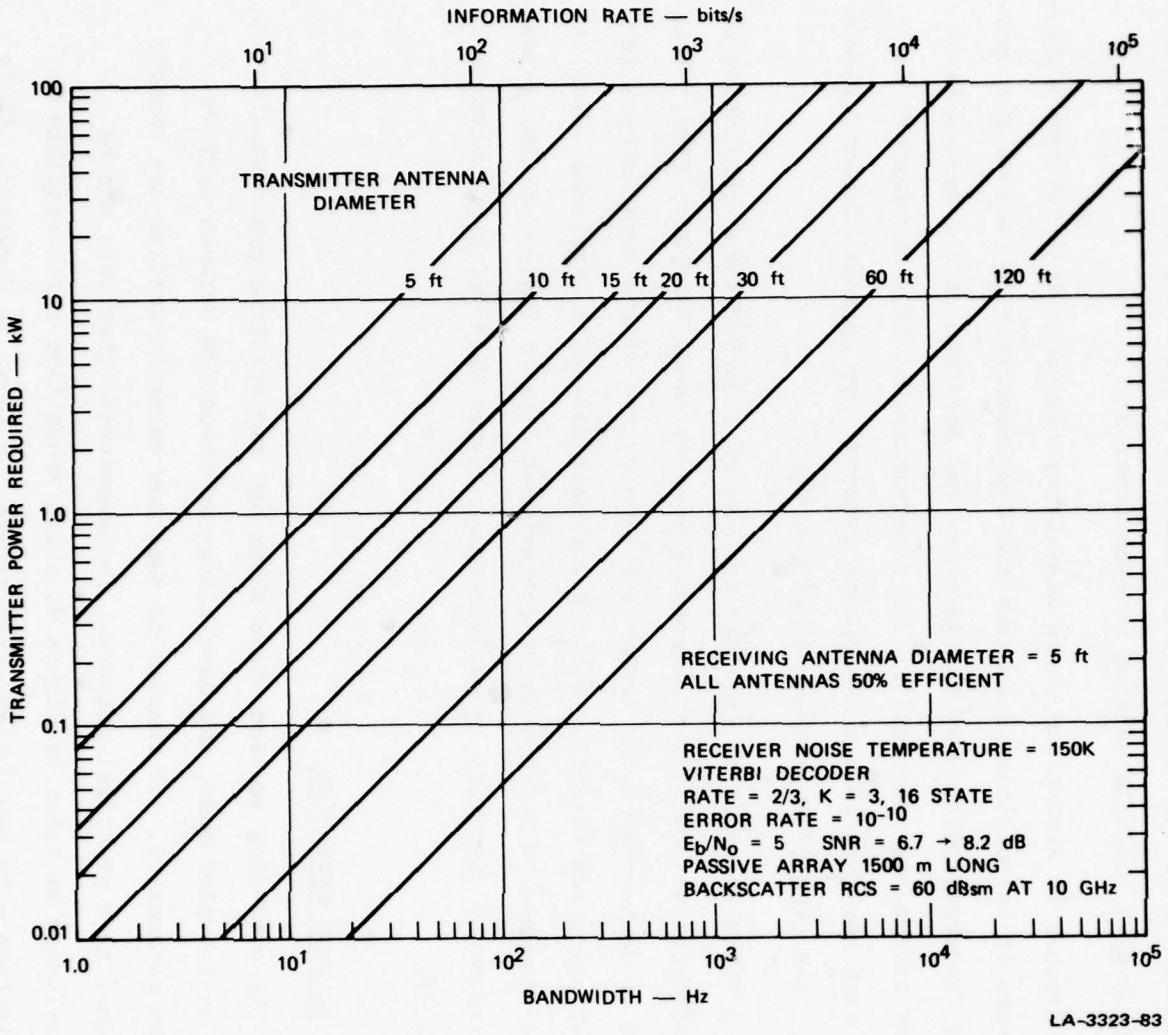

FIGURE 7 TRADEOFFS — FIVE-FOOT RECEIVING ANTENNA

the designer of a space-array system has several options available. First, he may use simple time-division multiplexing--i.e., delay the reply until reception of an incoming message is complete. This procedure is appropriate for emergency action messages and allows the use of a single array in combination with a single antenna at each terminal.

Second, in situations where many arrays are available through proliferation, it is possible to achieve two-way communication because the operating frequency depends on the geometry and location of the arrays (even if the arrays are identical). The disadvantage of this arrangement is that each terminal requires separate antennas for transmission and reception. The situation is shown in Figure 8(a).

A third possibility involves the use of a duplex array consisting of two sections with different array spacings as shown in Figure 8(b). This tends to double the array length but permits use of the same antenna for transmission and reception as with conventional earth stations. Finally, it is possible to achieve great operational flexibility by combining space and frequency diversity by proliferating arrays with different element spacings.

E. Network Operation

The preceding sections have shown how two stations can communicate in a full-duplex mode, and have discussed tradeoffs between various system parameters. It remains to show how several stations can operate together as a practical network. To demonstrate that this can be accomplished we refer to Figure 9, which shows five earth stations in combination with two duplex space arrays, as shown in Figure 8. It is clear that any particular earth station can direct its antenna to either satellite and can select a frequency that steers power to any one of the four remaining stations. It is unlikely that the illuminated

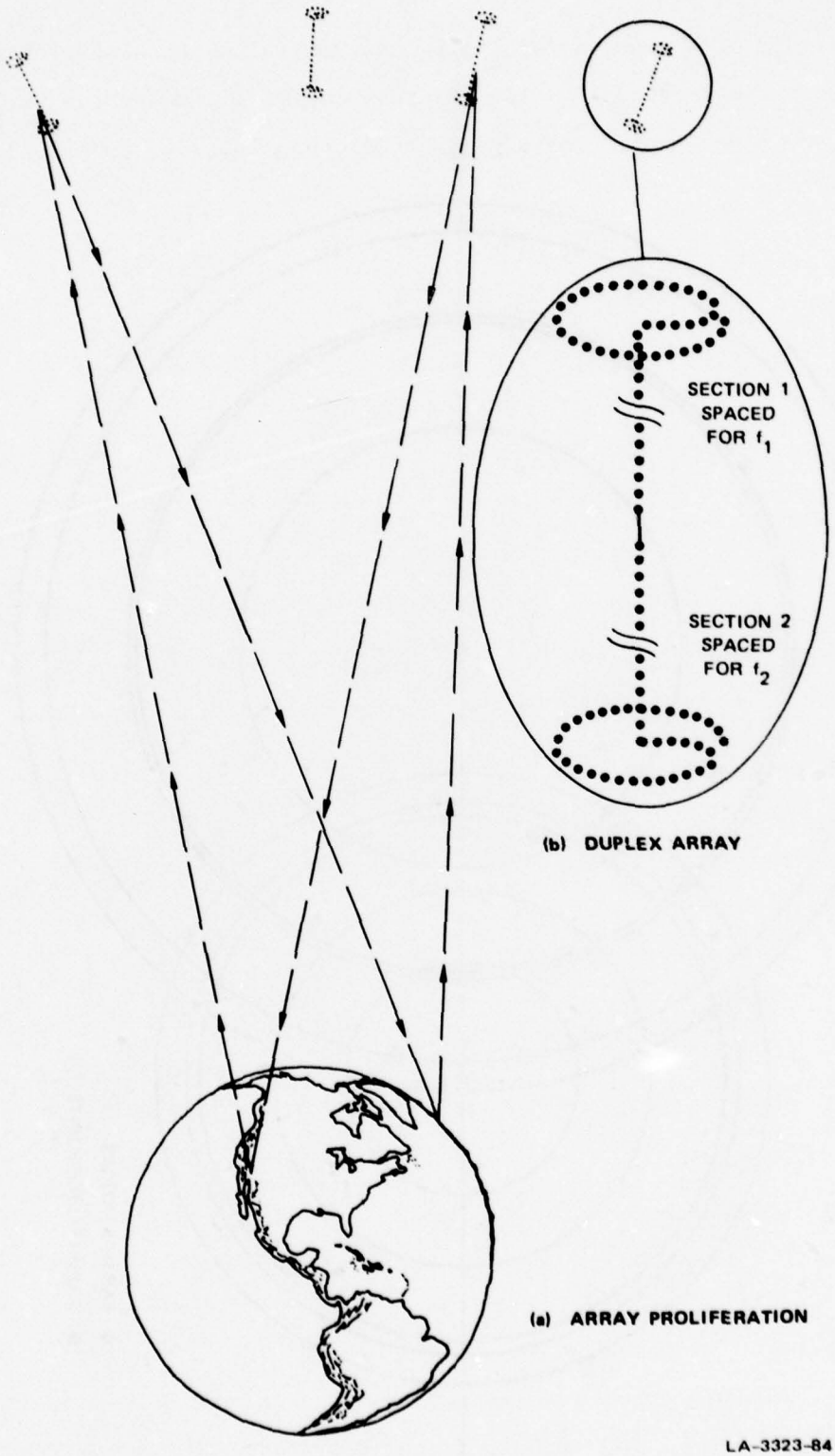

FIGURE 8 TWO-WAY COMMUNICATION METHODS

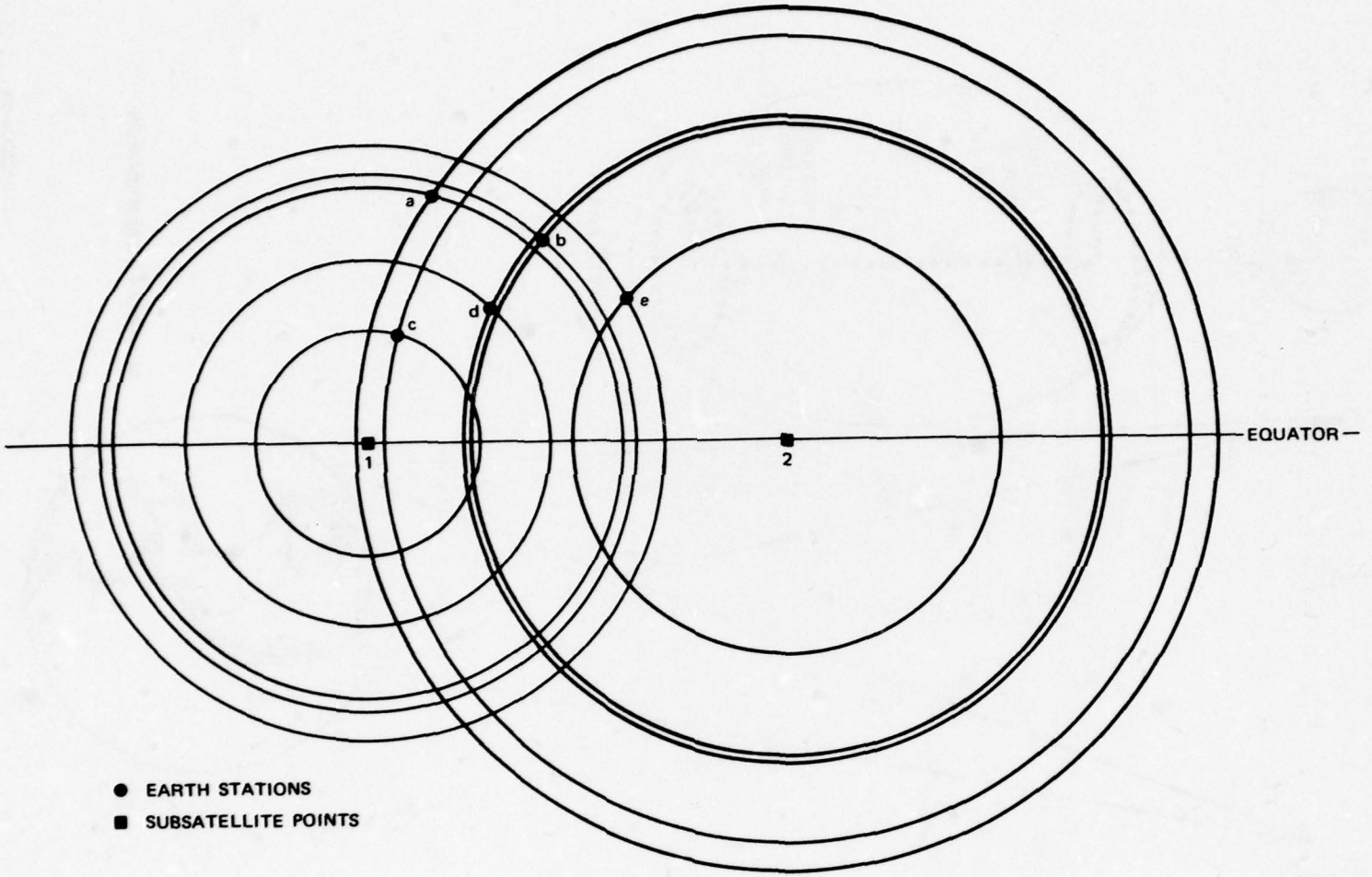

FIGURE 9 NETWORK GEOMETRY

annulus passing through the intended receiver station will also pass through any of the other three stations. This unlikely situation could be accommodated by time-division multiplexing, or could be avoided by shifting operation to the other satellite with an appropriate change of frequency.

Consideration of the geometrical and frequency choices available, together with the fact that the operating annulus has a width of only 10 km shows that each of the five stations will be able to communicate separately with any of the other four. In no reasonably probable situation will a station find that his transmissions simultaneously reach two of the other stations and that he cannot obtain relief by switching to the other satellite.

V VULNERABILITY

Preliminary calculations have been made to estimate the vulnerability of an aluminum sphere array to nuclear attack. They show that an array of aluminum spheres is most vulnerable to vaporization recoil due to x-rays, whereas active satellites are usually most vulnerable to neutrons. For this reason the most effective way of comparing the vulnerability of such dissimilar satellites is by a graph of range against weapon yield. A graph of that type appears as Figure 10. The principal conclusion that may be drawn from this graph is that any opponent will be forced into a one-on-one attack on the array, which is quite costly because passive

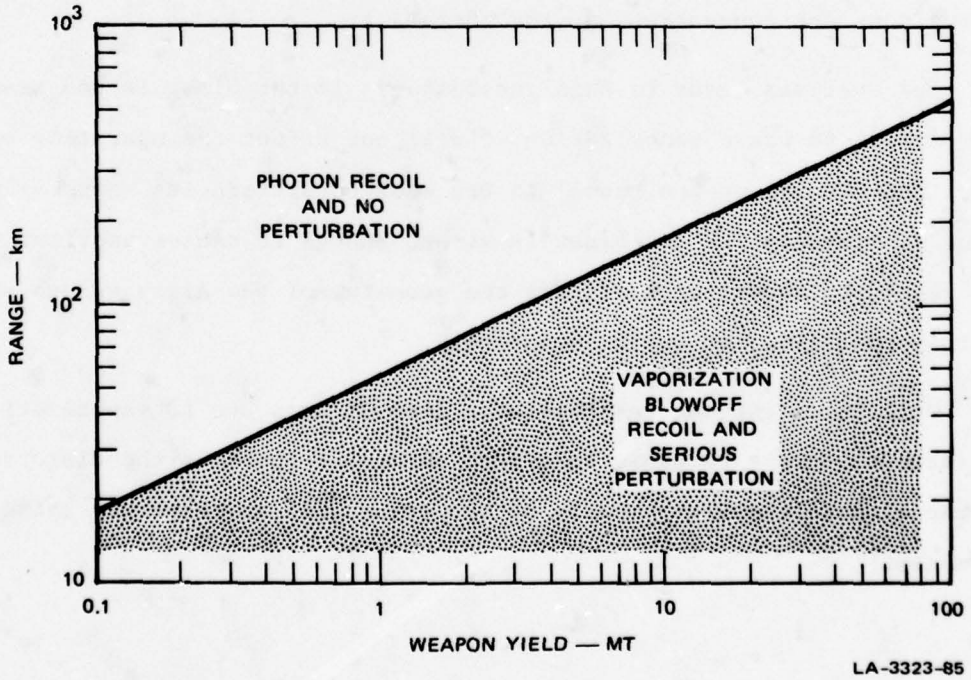

FIGURE 10 VULNERABILITY TO NUCLEAR ATTACK OF 1500 m ARRAY OF ALUMINUM SPHERES

arrays are relatively cheap and easy to proliferate, whereas high-yield nuclear weapons delivered at synchronous altitude are inevitably expensive.

The principal outputs of a nuclear weapon detonated in space are x-rays, high-velocity debris, gamma rays, beta rays, and neutrons. The dominant effect against the passive array are x-rays with energies of several kilovolts. At relatively large distances the only effect is a slight recoil due to their quantum momentum. At closer ranges or higher x-rays intensities, the surface temperature of the metal is raised sufficiently to produce vaporization. The forces due to recoil from vaporization are about four orders of magnitude larger than those produced by photon recoil. Therefore, boundary between photon recoil and recoil due to vaporization is the dominant feature of Figure 10. This criterion is independent of the array form but differs somewhat for different materials. Aluminum has favorable properties because x-rays penetrate it easily so that their energy does not concentrate at the surface.

Our analysis leads to this conclusion: If the blast is too weak and too distant to cause vaporization it will not affect the operation of the array because the photon recoil is too weak to disturb its shape or position. Conversely, if the blast is strong enough to cause vaporization, the resulting recoil will disturb the geometry of the array enough so that it is inoperative, at least temporarily.

Only in an extreme case will the loss of mass due to vaporization be sufficiently great to cause long-term damage. Otherwise the disruption of the signal-relaying property of the array will be temporary rather than permanent.

VI ORBITAL DYNAMICS

The orbital characteristics of the space array do not differ in any essential way from those of other satellites in synchronous orbit.* However, several topics differ in detail because of the unique configuration and relatively low mass-to-area ratio of the array. A synchronous orbit with little or no inclination is favored because it places minimum requirements on frequency steering and ground-station tracking. A very circular orbit is desired because eccentricity tends to cause libration of the array, which is difficult to control.

A. Gravity Gradient

Consider a satellite in the form of a long, slender rigid bar that is aligned with the local vertical so that it rotates around the earth (and with respect to space) once every 24 hours. The outer end of such a bar has a higher velocity and a greater centrifugal force than the inner end. Conversely, the inner end experiences a slightly stronger gravitational force because it is closer to the center of the earth. The combination of these influences causes the bar to have internal tension and to tend to align itself with the local vertical.

If perturbed from the vertical position the bar will oscillate or librate about it. The period of the libration perpendicular to the orbital plane is exactly half the orbital period. For a synchronous

---

*The material in this section is taken from a recent report on this project,[6] which should be consulted by anyone seeking more information on this topic.

satellite this period is 12 hours. Libration in the plane of the orbit has a slightly longer period--i.e., 24 hrs/$\sqrt{3}$, or approximately 14 hours.

If the rigid bar is replaced by a flexible member such as a cable or a chain the dynamic properties become considerably more complicated. In addition to librating as a straight member, the cable is capable of oscillating in various flexural modes, which are not restricted to a single plane. A few of these planar normal modes are illustrated in Figure 11. Fortunately, such flexural modes are subject to fairly rapid damping by the internal viscosity of the material, or by friction in physical joints. This property is exploited in the present satellite design, which damps the librational mode by coupling it to flexural modes.

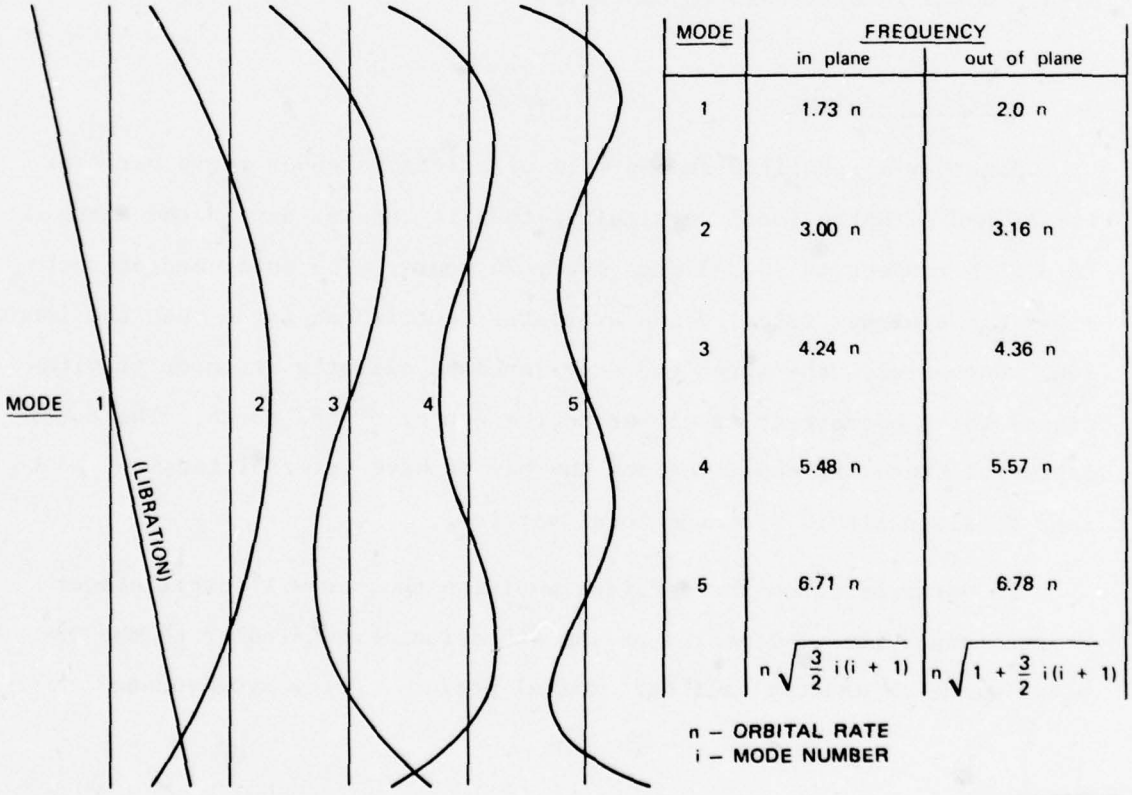

MODE	FREQUENCY	
	in plane	out of plane
1	1.73 n	2.0 n
2	3.00 n	3.16 n
3	4.24 n	4.36 n
4	5.48 n	5.57 n
5	6.71 n	6.78 n
	$n\sqrt{\frac{3}{2}\,i(i+1)}$	$n\sqrt{1+\frac{3}{2}\,i(i+1)}$

n – ORBITAL RATE
i – MODE NUMBER

LA-3323-61

FIGURE 11 GRAVITY-GRADIENT NORMAL MODES FOR FREE CABLE

The basic damping concept is illustrated in Figure 12, which shows a rigid bar, hinged through ball joints to a pair of tip devices that consist of a circular disk and a short shaft. The essential fact is that the

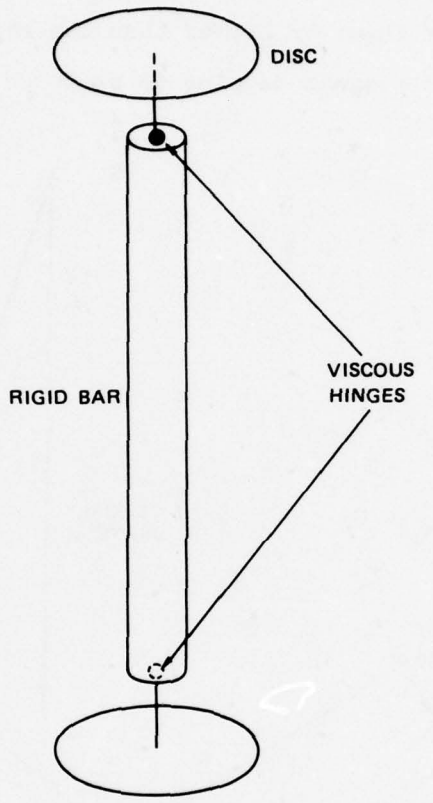

FIGURE 12 CONCEPTUAL DAMPING MODEL

libration properties of the tip devices differ from the libration properties of the straight bar. If such a system is released with arbitrary initial conditions, it will librate about the local vertical in a complicated three-dimensional pattern that includes substantial relative motion in both joints. The oscillation will be damped, and the equilibrium position will be approached as a result of friction in the joints.

The actual array is not rigid, but for purposes of analysis can be approximated by a flexible cable. Through analysis and modeling we have determined that tip inertia units of the type shown in Figure 12 are also effective when applied to a flexible cable. Figure 13 shows the shape that the cable will take when the tip proportions are chosen to tune the tip oscillation either lower or higher than the main libration period. Greatest flexure and strongest damping is produced in the tuned condition.

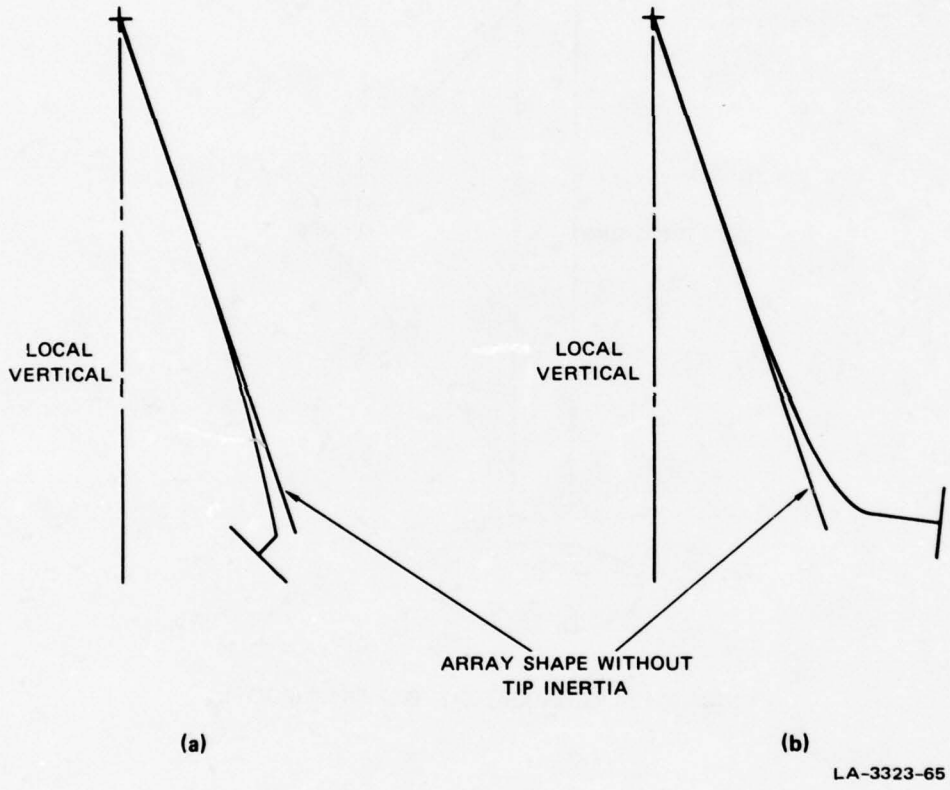

FIGURE 13 FIRST MODE SHAPES WITH TIP INERTIA

The actual array differs from this conceptual model in several details. First, to facilitate deployment, each tip-inertia unit consists of a single coil or pigtail of the same type as the general array, rather than being a separate disk as illustrated in Figure 13. Second, the main body of the array is not a rigid bar, but consists of a large number of

units connected by limited-motion joints. Friction in these joints produces additional damping of any flexural modes that may result from coupling between main-body libration and tip oscillation. The construction is shown in Figure 14.

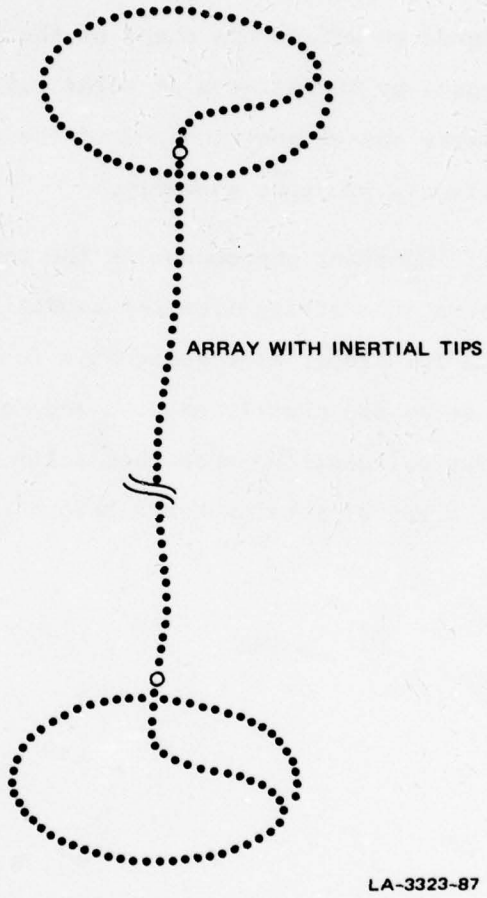

FIGURE 14 ARRAY WITH INERTIAL TIPS

B. Perturbing Influences

The orbit and attitude of any satellite is subject to perturbations or disturbances from a large number of influences. Of these, the most important one to our satellite is solar radiation pressure.

Solar radiation pressure affects the space-array satellite in two different ways. First, it tends to change an initially circular orbit into an elliptic orbit. The degree of ellipticity increases over a period of six months, then decreases through the next six months so that the orbit resumes its original form at the end of one year. Second, the solar radiation pressure tends to affect the shape of the array. A very light array would be collapsed by the effects of solar radiation pressure if the sun were in a nearly end-on position and if the array initially was distorted from a perfectly straight geometry.

Perhaps the most important phenomenon is the tendency of solar radiation pressure to distort the array, from the condition of nearly perfect straightness required for proper electromagnetic functioning, unless all the elements of the array are equally massive and respond equally to solar radiation forces. Our calculations show that solar radiation pressure will not distort the array of metal spheres beyond acceptable tolerance limits.

VII LAUNCH AND DEPLOYMENT

Before the array can serve as a communication satellite it must first be successfully launched and deployed. These topics are discussed in the following paragraphs.

A. Launch

For a piggyback launch to synchronous altitude, the best opportunity that has been found is a Titan III-C rocket dedicated to the launch of a pair of 777 satellites during the latter half of 1977. As it approaches synchronous altitude this vehicle consists of a power transport stage (transtage) and the two satellites, which are stacked one above the other and have their own station-keeping capability.

A substantial amount of space exists between the lower 777 and the transtage. We propose to store the space-array deployment package in this space, which has the boundaries shown in Figure 15. The general configuration of the transtage with payloads and the contemplated deployment sequence are shown in Figure 16. The sequence shown differs from the conventional sequence only by the presence of the passive array payload and by one additional reorientation to deploy it.

B. Deployment

Ideally, the array should be deployed in such a way that it would be straight, aligned with the local vertical, and rotating once a day so as to remain earth pointing. It should also be tranquil--i.e., free from internal velocities or motions. Such an ideal deployment is unlikely in practice, but should be approximated as closely as possible. The

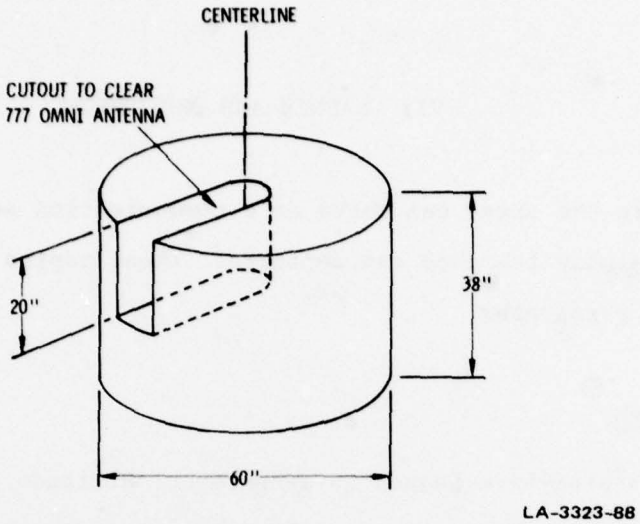

FIGURE 15 TITAN III-C AVAILABLE VOLUME FOR PIGGYBACK

deployment mechanism that has been chosen to achieve these requirements is shown in Figure 17. The array is stored in a circular canister or chain locker and is suitably constrained so that the vibrations encountered during the launch will not injure the array or its associated mechanisms. Between launch and deployment the constraint is released and the array is tranquil within the container. When the launch command is received the pair of sprockets is accelerated to a surface velocity of a few meters per second and the array is ejected toward the nadir. The deployment process ends when the array leaves the deployment sprockets. The deployment process causes the orbit of the array to differ somewhat from that of the launch vehicle at the time of launch. However, the difference is smaller than the orbit uncertainty of the parent vehicle, so the effect is unimportant.

The deployment process is complicated by the stabilization dynamics of the transtage of the Titan III-C rocket. The transtage is subject to three-axis stabilization, which holds the axes accurate to within approximately $\pm 1/2°$. However, the motor impulses that produce this stabilization

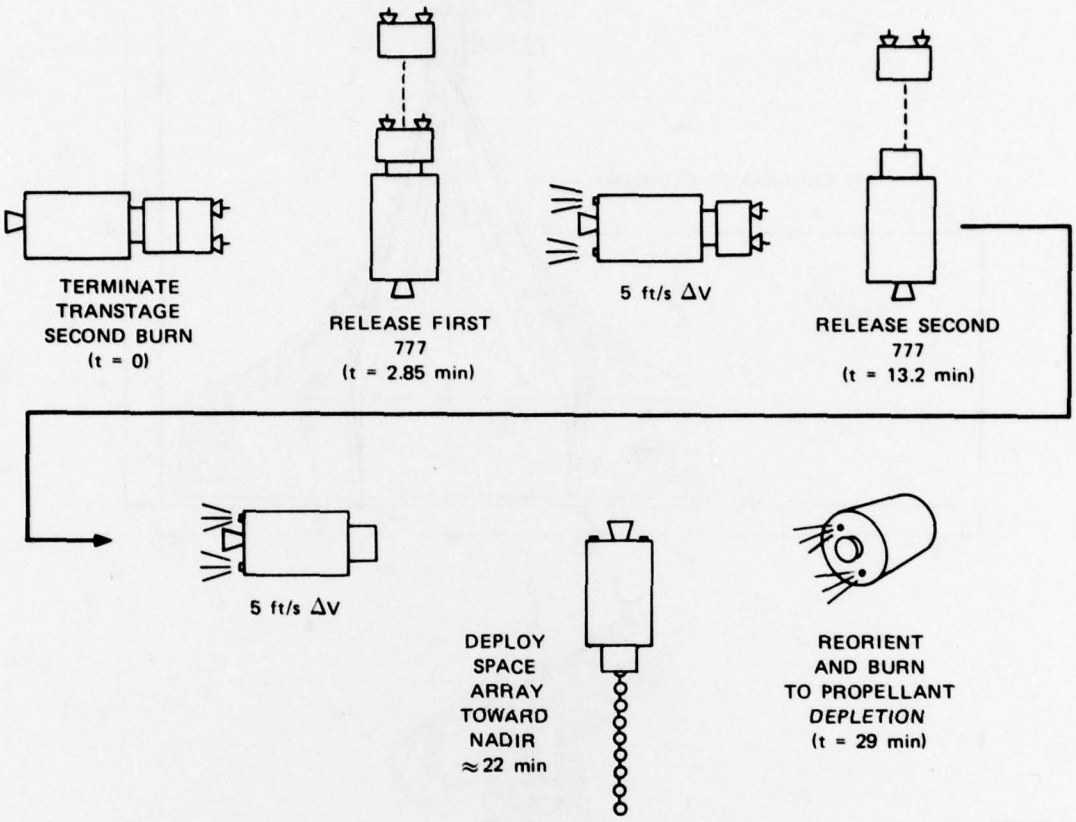

FIGURE 16 REPRESENTATIVE DEPLOYMENT SEQUENCE

are not under precise control. Therefore the process includes a considerable degree of randomness. Such disturbances tend to cause the array to be ejected in a sinuous rather than the desired straight-line manner. The oscillation energy imparted to the array might cause it to collapse if suitable measures were not taken. The principal measure that has been taken to overcome this difficulty is to make the array of sections that are inherently stiff and to connect them by limited-motion joints. In this way the tendency to collapse is overcome, and the energy imparted by the transtage cycling is transformed into bending potential energy in the array. The latter energy is subsequently dissipated by viscous friction in the array joints. Figure 18 shows the attitude-control system,

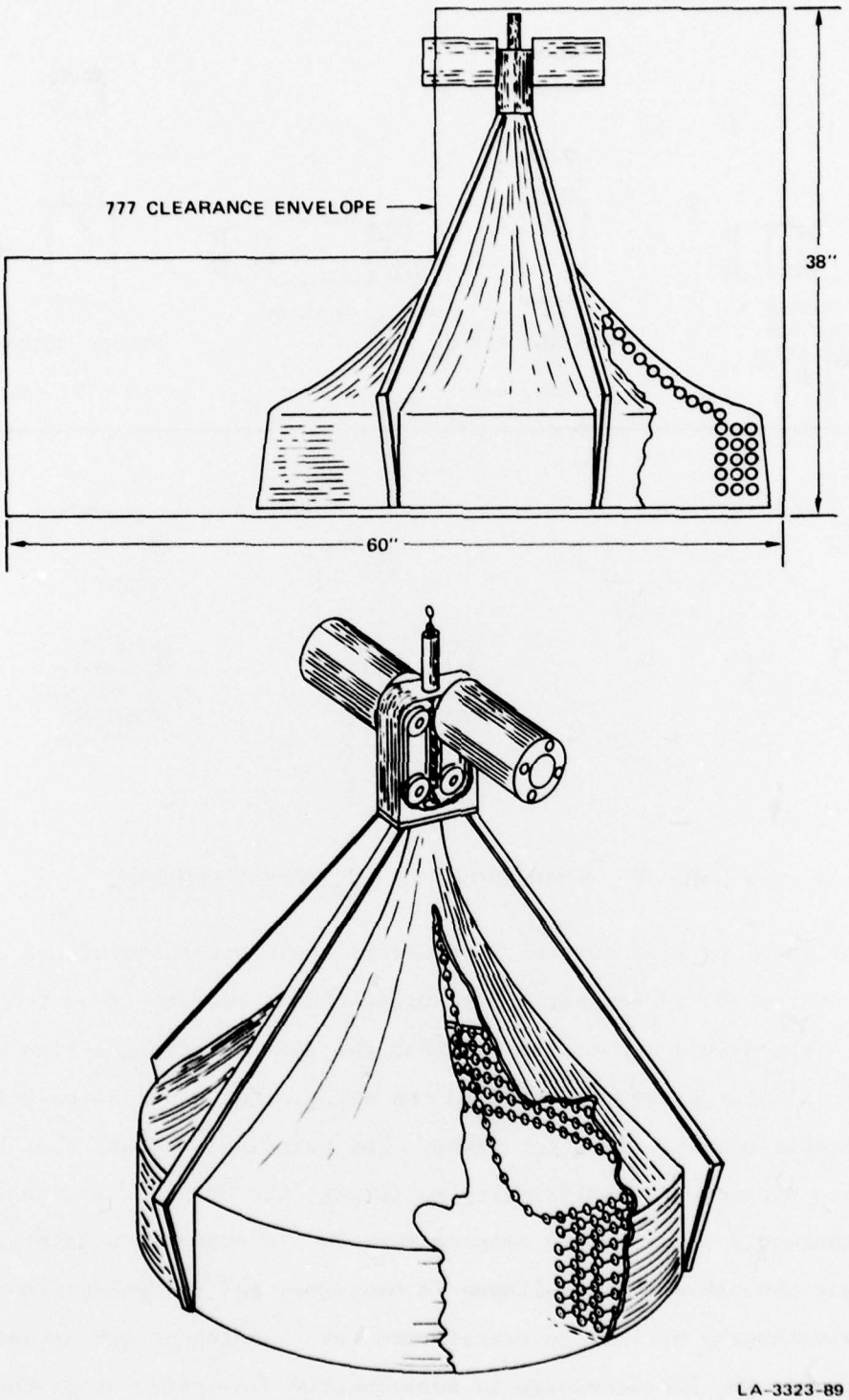

FIGURE 17 DEPLOYMENT MECHANISM

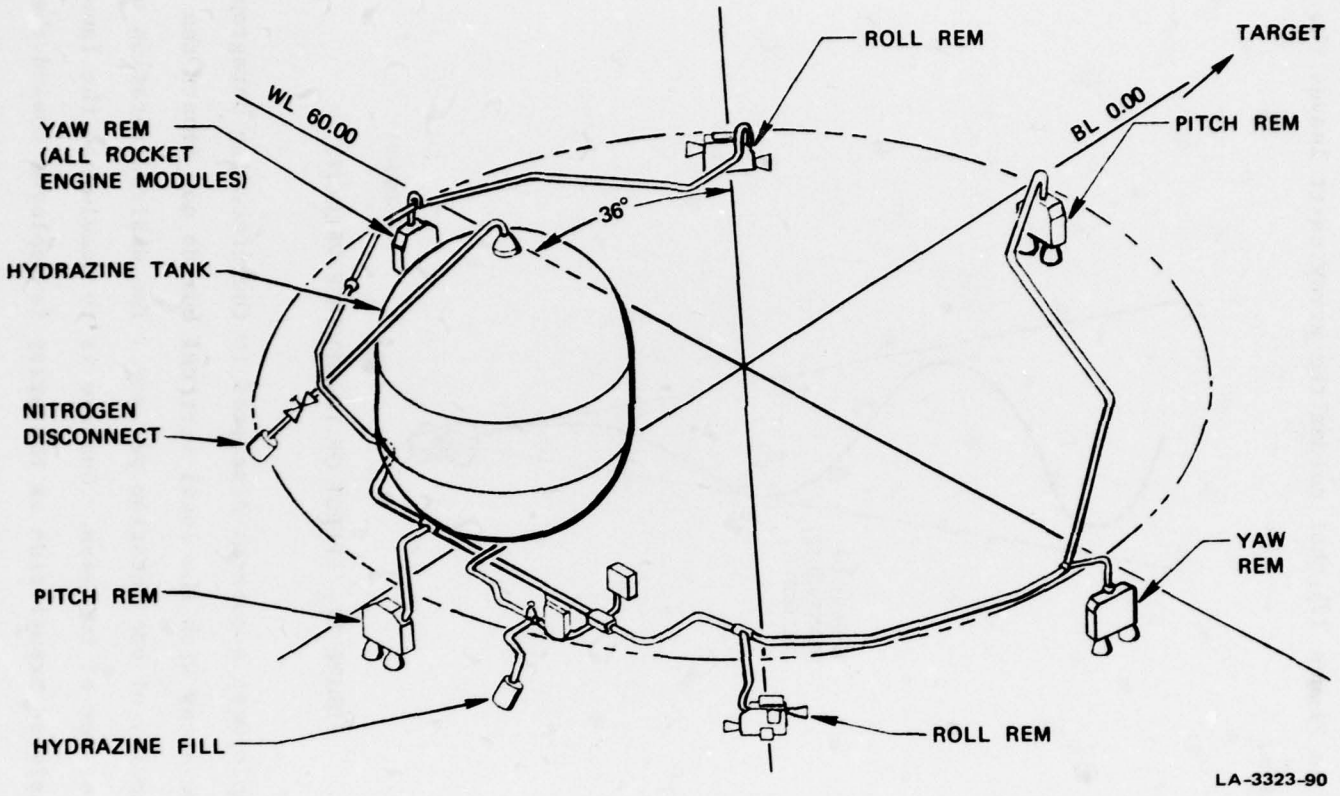

FIGURE 18 TITAN III-C ATTITUDE CONTROL SYSTEM

and Figure 19 shows how the deployment tends to be affected. This tendency can be overcome by adding gyroscopic or servo control to the exit tube (shown in Figure 17) that guides the array as it leaves the deployment mechanism.

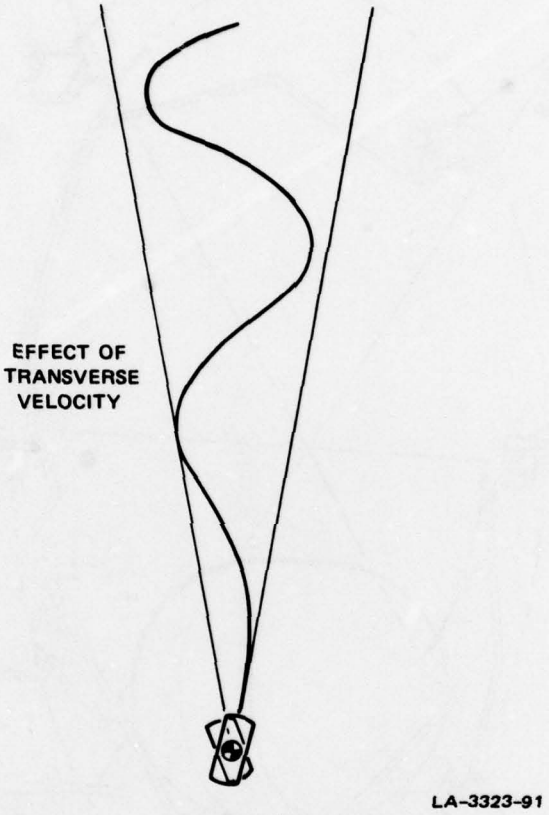

FIGURE 19 EFFECT OF TRANSVERSE VELOCITY

The deployment sequences discussed in the preceding paragraphs tend to align the array with the local vertical but do not impart the needed angular velocity of one rotation per day. The desired rotation can be secured in either of two ways. One way is to accelerate the launch vehicle in eastward translation as the array is deployed toward the nadir. This will generate the needed difference in velocity between the upper and lower tips of the array. The other option is to rotate the transtage

during deployment in the direction opposite to that desired for the array. The changing angle of ejection during deployment produces the necessary changes of velocity, thereby inducing the desired rotation.

The first option requires a velocity difference of about one cm/s between the two ends of the array. The second option requires a (negative) rotation rate of one turn per day with respect to the fixed stars or a negative and twice the orbital rate with respect to a rotating frame of reference.

The attitude control mechanism cannot provide accuracies of this degree on a short-term basis. However, the attitude sensors are highly accurate. Therefore, we can obtain the needed precision by programming and averaging the controls over the many cycles that occur during the deployment interval.

VIII ARRAY CONSTRUCTION

Figure 20 shows the manner in which the array is to be fabricated. The working portion of the array will consist of 100 sections that are individually straight, and 1.5 m long. Adjacent sections are joined by limited-motion ball-joint connectors that are very free for motions below approximately 3° but are stiff for larger motions. Each joint is filled with a viscous damping fluid that provides freedom to very slow motions but absorbs energy associated with oscillatory motion. Perchlorinated poly-ether is one of several materials being considered for use as the damping fluid.

The end sections are made in the same way as the rest of the array but do not contain joints. They are prestressed so that they will assume the desired circular pigtail configuration after deployment, when they are subject to the very weak gravity-gradient forces. In each transition region where the straight section of the array joins the tip-inertia sections there are several special joints having a higher degree of motion so that the tip-inertia section can rock to total angles of approximately 70° with respect to the straight portion of the array. Large angular motion is contemplated because the deliberately introduced tuning of the tip inertia will enhance or magnify the motion of the tip compared to the libration of the overall array.

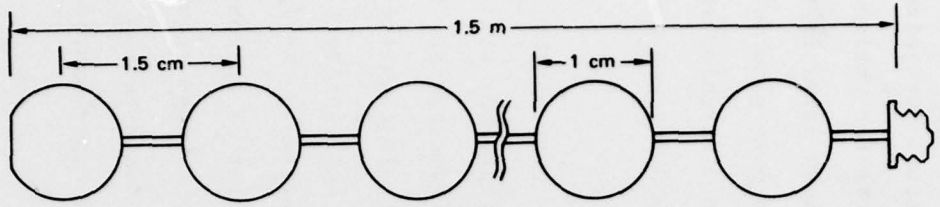

TYPICAL SECTION OF ARRAY

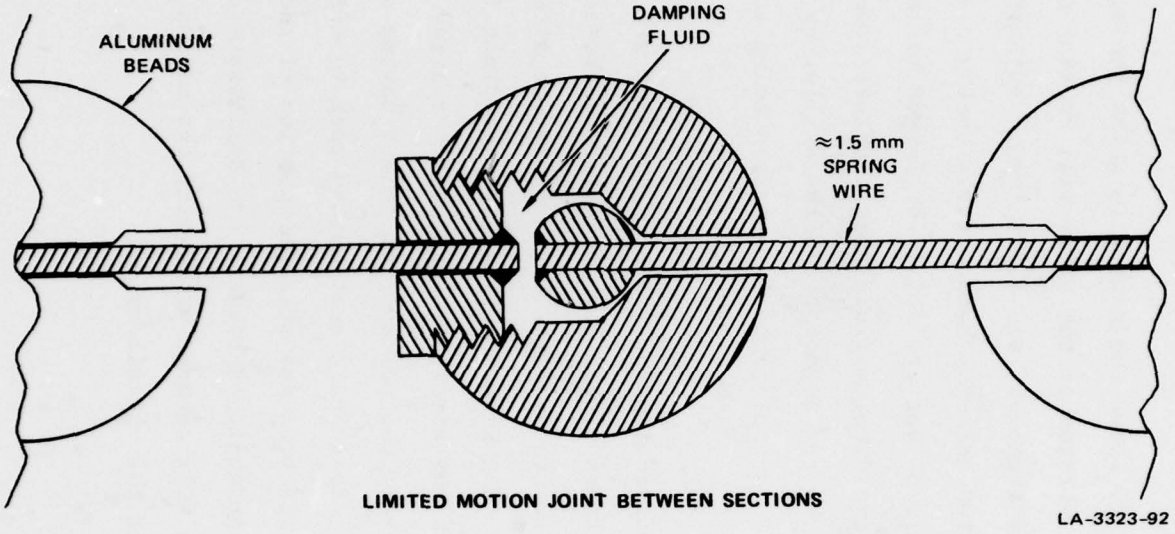

FIGURE 20 ARRAY CONSTRUCTION

IX STATUS AND CONCLUSIONS

The electromagnetic properties of the array have been determined by analysis and computer modeling, and have been confirmed by a series of experiments on arrays including as many as one thousand beads. Tests of longer arrays near the surface of the earth is infeasible because of difficulties in maintaining straightness and because it requires considerably more than a mile to reach the far-field region of a full-length array. Measurement of the far-field electrical scattering properties of an array of 10,000 beads is thus one important objective of a space experiment.

Jam resistance is one of the most important properties of the array. This property is strongly dependent on the high-order sidelobes of the array, which tend to be controlled by small departures of the array from its ideal configuration. Measurements to confirm that the array has the predicted jam resistance are another important objective of the feasibility demonstration experiment.

The orbital and attitude behavior of the array has been studied through analysis and computer simulation. This work indicates that the array will be stable in orbit, and will maintain the desired attitude. Libration has been identified as the principal form of motion that is likely to cause difficulty. Analysis and modeling indicate that the chosen array configuration (straight center section with pigtail tips) will be able to damp out such librations. However, the forces involved are too small to measure on earth, and a space environment test is necessary to confirm these results.

A mechanism for deploying the array from the transtage of a Titan III-C vehicle has been designed, and preliminary tests indicate that the

mechanism will meet the requirements of the system. Attitude cycling of the depleted transtage is the principal obstacle to a successful deployment. The array has been stiffened and other steps are being taken to mitigate such disturbances. The status of the program and the work that has been done have been reviewed with personnel of numerous agencies, including SAMSO, Aerospace, Martin Marietta, Applied Physics Laboratory, University of California, Lincoln Laboratory, DCA, ARPA, and DTAACS. These reviews have disclosed no fundamental flaw in the proposed experiment. However, the feasibility of the method can ultimately be demonstrated only by a space experiment. For these reasons it appears that the next step is to build and launch an array.

Figure 21 shows the time schedule proposed for accomplishment of the spacecraft coordination and related tasks. Figure 22 shows the schedule for all of the activities that must be accomplished within the overall time framework of the project.

- TIME SCHEDULE

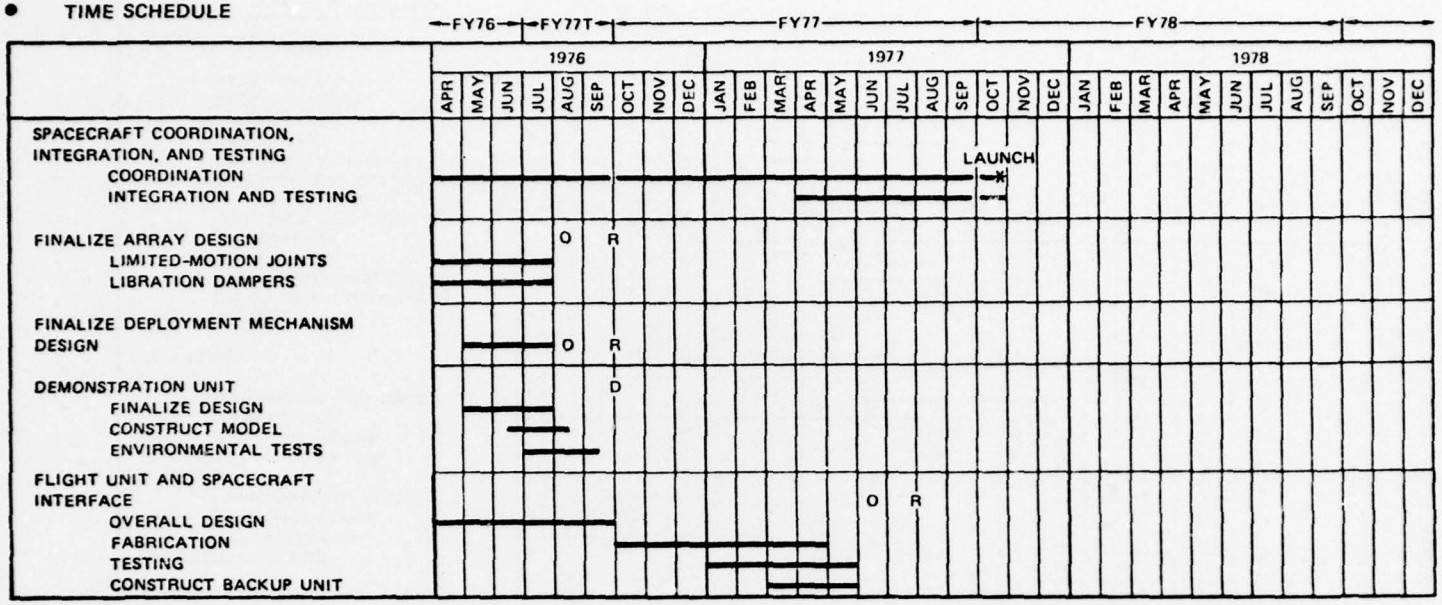

- FLIGHT UNIT AND SPACECRAFT INTERFACE
  - — PRELIMINARY-DESIGN REVIEW MEETING FOR FLIGHT UNIT — 30 APRIL 1976
  - — FINAL-DESIGN REVIEW MEETING FOR FLIGHT UNIT — 16 AUGUST 1976
  - — OVERALL DESIGN OF FLIGHT UNIT AND INTERFACE HARDWARE — 30 SEPTEMBER 1976
  - — FABRICATION OF FLIGHT UNIT AND INTERFACE HARDWARE — 30 APRIL 1977
- FINAL SPACE QUALIFICATION TESTS OF FLIGHT UNIT AND INTERFACE HARDWARE — MAY 1977
- INTEGRATION OF SPACE ARRAY PACKAGE TO LAUNCH VEHICLE — APRIL TO OCTOBER 1977
- LAUNCH — OCTOBER 1977

LA-3323-93

FIGURE 21 SPACECRAFT COORDINATION AND RELATED TASKS

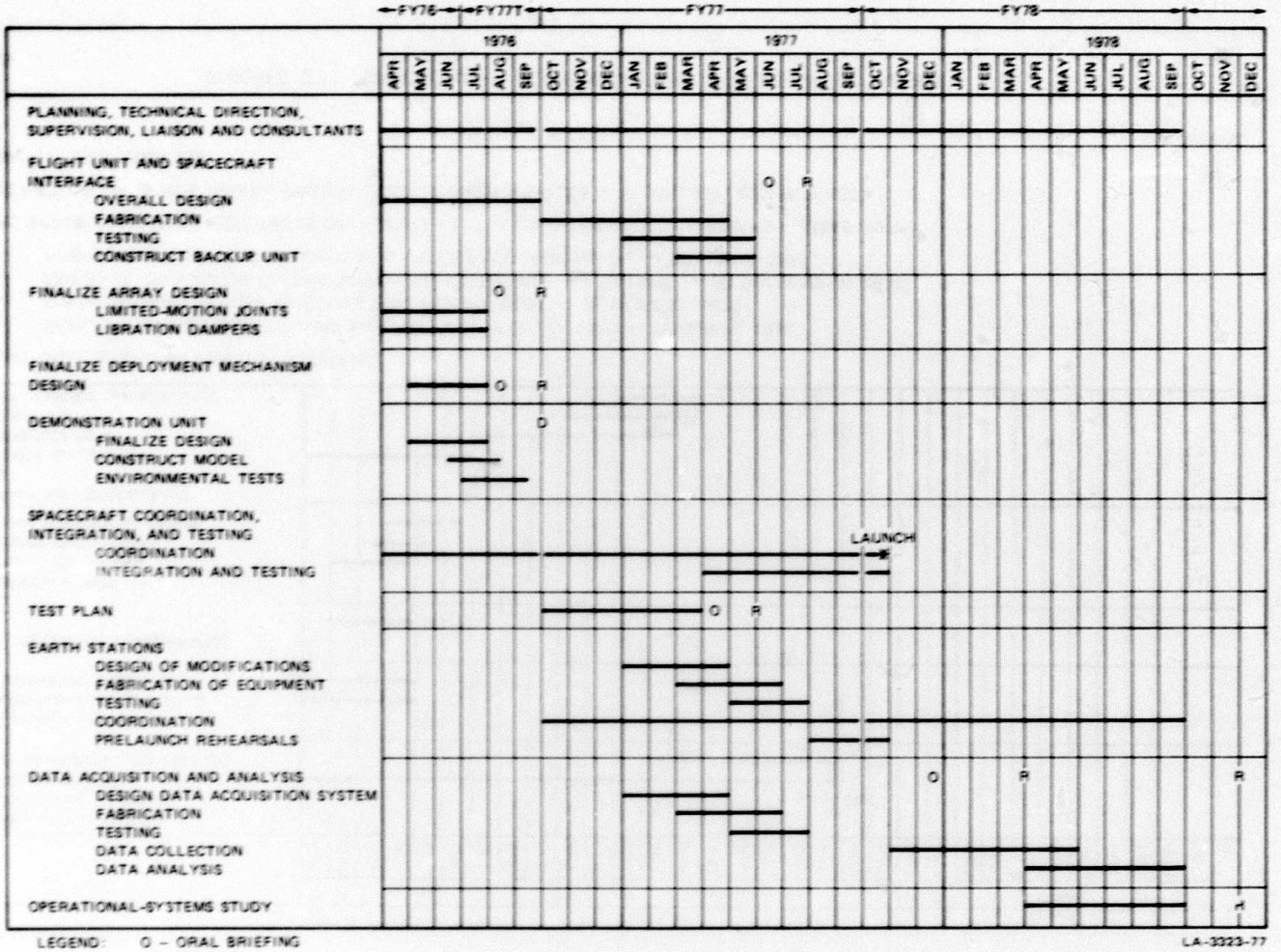

FIGURE 22 MILESTONE CHART

REFERENCES

1. J. C. Yater, "Signal Relay Systems Using Large Space Arrays," IEEE Trans. on Communications, Vol. COM-20, No. 6, pp. 1108-1121 (December 1972).

2. J. C. Yater, "Communication Satellite," U.S. Patent No. 3,427,623, issued 11 February 1969.

3. M. S. Frankel and T. L. Adams, "Electromagnetic Properties of a Passive Space Array," Special Tech. Report 2, Contract DCA100-74-C-0035, SRI Project 3323, Stanford Research Institute, Menlo Park, California (January 1975).

4. J. D. Kraus, Antennas (McGraw Hill Book Company, New York, New York, 1950).

5. M. S. Frankel, "The Fabrication and Test of a Long Array Segment," Special Tech. Report 4, Contract DCA100-74-C-0035, SRI Project 3323, Stanford Research Institute, Menlo Park, California (October 1975).

6. G. B. Andeen, "Orbital, Attitude, and Deployment Considerations for a Passive Space Array," Special Tech. Report 5, Contract DCA100-74-C-0035, SRI Project 3323, Stanford Research Institute, Menlo Park, California (December 1975).